

Entanglement renormalization in noninteracting fermionic systems

G. Evenbly and G. Vidal

School of Mathematics and Physics, The University of Queensland, Brisbane 4072, Australia

(Received 18 December 2009; revised manuscript received 30 April 2010; published 2 June 2010)

We demonstrate, in the context of quadratic fermion lattice models in one and two spatial dimensions, the potential of entanglement renormalization (ER) to define a proper real-space renormalization group transformation. Our results show the validity of the multiscale entanglement renormalization ansatz to describe certain ground states in two dimensions, including quantum critical states. They also unveil a connection between the performance of ER and the logarithmic violations of the boundary law for entanglement in systems with a one-dimensional Fermi surface. ER is recast in the language of creation/annihilation operators and correlation matrices.

DOI: [10.1103/PhysRevB.81.235102](https://doi.org/10.1103/PhysRevB.81.235102)

PACS number(s): 05.50.+q, 03.67.Mn, 05.10.Cc, 05.70.Jk

I. INTRODUCTION

The *renormalization group* (RG), concerned with the change of physics with the observation scale, is among the main ideas underlying the theoretical structure of statistical mechanics and quantum field theory and is of central importance in the modern formulation of critical phenomena and phase transitions.¹ Its influence extends well beyond the conceptual domain: RG transformations are also the basis of numerical approaches to the study of strongly correlated many-body systems.

In a lattice model, a real-space RG transformation produces a coarse-grained system by first joining the lattice sites into blocks and then replacing each block with an effective site.² Two very natural requirements for a RG transformation are (i) it should preserve the long-distance physics of the system; and (ii) when this physics is invariant under changes of scale, the system should be a fixed point of the RG transformation.

For the important case of a quantum system at zero temperature, the first requirement is fulfilled if, as determined by White in his density matrix renormalization group (DMRG),³ the vector space of the effective site retains the local support of the ground state. *Entanglement renormalization* (ER) (Ref. 4) has recently been proposed in order to simultaneously meet the second requirement. By using *disentangles*, ER aims to produce a coarse-grained lattice locally identical to the original one in the sense that their sites have the same vector space dimension. When this is accomplished, the original system and its coarse-grained version can be meaningfully compared, e.g., through their Hamiltonians or ground-state properties, leading to a proper real-space RG flow.

Promisingly, ER has been successfully demonstrated for the one-dimensional (1D) quantum Ising model with transverse magnetic field, where it has been shown that, indeed, at the quantum critical point the system is invariant under the resulting RG transformation.⁴ However, plenty of work is still required to characterize the main features and range of applicability of this new approach and, in particular, it remains to be seen whether ER also works in the computationally more challenging context of two-dimensional (2D) lattice systems, where DMRG can no longer analyze large systems.

In this paper we explore the performance of ER in systems of spinless fermion both on 1D and 2D lattices, as specified by the quadratic Hamiltonian

$$\hat{H} = \sum_{\langle rs \rangle} [a_r^\dagger a_s + a_s^\dagger a_r - \gamma(a_r^\dagger a_s^\dagger + a_s a_r)] - 2\lambda \sum_r a_r^\dagger a_r, \quad (1)$$

where λ and γ are the chemical and pairing potentials and the first sum involves only nearest neighbors. In spite of its simplicity, Hamiltonian \hat{H} contains a rich phase diagram as a function of λ and γ , including insulating, conducting, and superconducting phases.⁵ Importantly, the corresponding ground states span all known forms of entropy scaling.^{5,6} In addition, \hat{H} can be diagonalized through linear (Fourier and Bogoliubov) transformations of the fermion operators \hat{a} and \hat{a}^\dagger while, by Wick's theorem, all properties of its *Gaussian* ground state $|\Psi_{\text{GS}}\rangle$ can be extracted from the two-point correlators $\langle \hat{a}_r^\dagger \hat{a}_s \rangle$ and $\langle \hat{a}_r \hat{a}_s \rangle$. Then, provided that our RG transformation also maps fermion modes linearly, the entire analysis can be conducted in the space of two-point correlators and quadratic Hamiltonians of N fermionic modes, as represented by $N \times N$ matrices. Hence quadratic fermionic models such as Eq. (1) offer an appealing testing ground for ER, one where computational costs have been greatly simplified [e.g., \hat{H} can be diagonalized exactly with just $O(N^3)$ operations] while keeping a rich variety of nontrivial ground-state structures.

II. COARSE-GRAINING NONINTERACTING FERMION SYSTEMS

We start by rephrasing, in the language of correlation matrices, the process of coarse graining a D -dimensional (hypercubic) lattice. We assume that the system is in the ground state $|\Psi_{\text{GS}}\rangle$ of \hat{H} , which we compute using standard analytic techniques.⁵ It is convenient to redraw the hypercubic lattice so that each site contains $P \equiv p^D$ fermion modes for some integer p . Then a hypercube of 2^D sites defines a *block* that contains $P2^D$ modes. The goal of the RG transformation is to replace this block with just one effective site made of P' modes, with $P' < P2^D$. We would like to have $P' = P$ so that the sites of the coarse-grained and original lattices are identical and we can compare the corresponding Hamiltonians or

ground-state reduced density matrices. However, in the coarse-graining step only modes of the block that are disentangled from the rest of the system can be removed. As a result, P' often must be larger than P .

For the sake of simplicity, we continue the analysis for the case of a 1D lattice. Let us temporarily replace the N spinless fermion operators \hat{a} in Eq. (1) with $2N$ (self-adjoint) Majorana fermion operators \check{c} ,

$$\check{c}_{2r-1} \equiv \hat{a}_r + \hat{a}_r^\dagger, \quad \check{c}_{2r} \equiv \frac{\hat{a}_r - \hat{a}_r^\dagger}{i}. \quad (2)$$

The ground state $|\Psi_{\text{GS}}\rangle$ is then completely specified by

$$\langle \check{c}_r \check{c}_s \rangle = \delta_{rs} + i\Gamma_{rs}, \quad (3)$$

where Γ , henceforth referred to as the *correlation matrix*, is real and antisymmetric. Similarly, the reduced density matrix ρ_{GS} for a block made of two sites, that is, with $L=2P$ spinless modes (equivalently, $2L$ Majorana modes) is described by a $2L \times 2L$ submatrix Γ_L of Γ . This matrix is brought into (block) diagonal form by a special orthogonal transformation V ,

$$V\Gamma_L V^\dagger = \bigoplus_{r=1}^L \begin{bmatrix} 0 & v_r \\ -v_r & 0 \end{bmatrix}, \quad V \in \text{SO}(2L), \quad (4)$$

where $0 \leq v_r \leq 1$ are the eigenvalues of Γ_L , each one associated with a pair of Majorana fermions. These pairs recombine into L spinless fermions in a product state¹⁰

$$\rho_{\text{GS}} = \bigotimes_{r=1}^L \varrho_r = \bigotimes_{r=1}^L \begin{pmatrix} \frac{1+v_r}{2} & 0 \\ 0 & \frac{1-v_r}{2} \end{pmatrix}, \quad (5)$$

where ϱ_r , the state of a spinless fermion mode, is *mixed* if $v_r < 1$ and *pure* if $v_r = 1$. Notice that since the ground state $|\Psi_{\text{GS}}\rangle$ is a pure state, a mode in a mixed state must be *entangled* with modes outside the block, whereas a mode in a pure state is *unentangled* from the rest of the system. We build an effective site by removing from the block, or *projecting out* from Γ_L , all the modes that are unentangled (pure), and just keeping those P' modes that are entangled (mixed). In this way, the coarse-grained lattice retains the ground-state properties.

III. ENTANGLEMENT RENORMALIZATION APPLIED TO NONINTERACTING FERMIONS

The key idea of ER, see Fig. 1, is to use disentangling unitary transformations, or *disentanglers*, to diminish P' by increasing the number of modes in the block that are unentangled from the rest of the system. A disentangler is implemented through a special orthogonal matrix $U \in \text{SO}(2L)$ that acts on two neighboring sites across the boundary of the block, whereas the coarse graining is implemented by an isometry $W = RY_{P'}$, that selects the P' spinless fermion modes to be kept in the effective site, where $R \in \text{SO}(2L)$ and

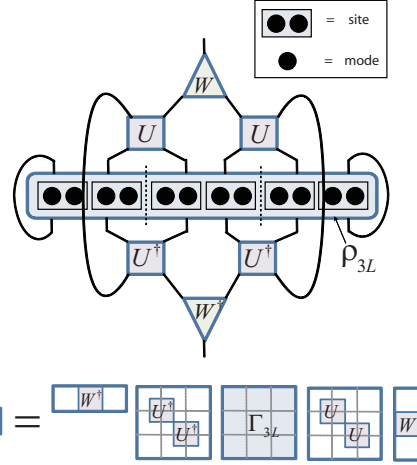


FIG. 1. (Color online) Top: a block of two sites (four modes) is coarse grained into an effective site by first applying disentanglers U across the boundary of the block and then using isometry W to project out two modes. Bottom: same RG transformation written in the language of correlation matrices, Eq. (7).

$$Y_{P'} \equiv \bigoplus_{r=1}^L \begin{bmatrix} 0 & g_r \\ -g_r & 0 \end{bmatrix}, \quad g_r = \begin{cases} 1 & r \leq P' \\ 0 & r > P' \end{cases}. \quad (6)$$

Let Γ_{L3} describe three consecutive blocks. Then the correlation matrix Γ'_L for the effective site reads (Fig. 1)

$$\Gamma'_L = W^\dagger (U \oplus U)^\dagger \Gamma_{3L} (U \oplus U) W. \quad (7)$$

Similarly, the correlation matrix $\bar{\Gamma}'_L$ for the modes to be removed is

$$\bar{\Gamma}'_L = \bar{W}^\dagger (U \oplus U)^\dagger \Gamma_{3L} (U \oplus U) \bar{W}, \quad (8)$$

$$\bar{W} \equiv R(Y_L - Y_{P'}), \quad Y_L \equiv \bigoplus_{r=1}^L \begin{bmatrix} 0 & 1 \\ -1 & 0 \end{bmatrix}. \quad (9)$$

Our goal is to maximize the *purity* of the modes to be projected out so that they become as unentangled as possible. The sum of their purities, $\sum_{r=P'+1}^L v_r$, is half of the antisymmetric trace of $\bar{\Gamma}'_L$, $\text{tr}(\bar{\Gamma}'_L Y_L^\dagger)$. Consequently, U and W are obtained from the optimization

$$\max_{U, R \in \text{SO}(2N)} \text{tr}(\bar{\Gamma}'_L Y_L^\dagger) \quad (10)$$

that we address through a sequence of alternating optimizations for U and R .¹¹

Then, given the correlation matrix Γ for $|\Psi_{\text{GS}}\rangle$, the RG transformation is implemented in three steps: (i) first a submatrix Γ_{3L} for three consecutive blocks is extracted from Γ ; (ii) then disentangler U and isometry W are computed using the optimization [Eq. (10)] while keeping $P'=P$ modes in the effective site; (iii) finally, U and W are used to transform the original N -mode system into a coarse-grained system with just $N/2$ modes and effective correlation matrix $\Gamma^{(1)}$. Some of the modes that are removed are still slightly mixed. Their mixness $\epsilon_r \equiv 1 - v_r$ quantifies the errors introduced. Iteration of the RG transformation produces a sequence of

increasingly coarse-grained lattices, described by correlation matrices $\{\Gamma^{(1)}, \Gamma^{(2)}, \dots\}$. The corresponding disentanglers $\{U^{(1)}, U^{(2)}, \dots\}$ and isometries $\{W^{(1)}, W^{(2)}, \dots\}$ constitute the *multiscale entanglement renormalization ansatz* (MERA) (Ref. 7) for the ground state $|\Psi_{\text{GS}}\rangle$.

IV. NUMERICAL RESULTS

We have applied the present RG approach to Hamiltonian of Eq. (1) in the thermodynamic limit $N \rightarrow \infty$. First we consider 1D systems, where the whole (γ, λ) plane can be mapped into the quantum spin XY model using a Jordan-Wigner transformation. (i) For the line $\gamma=1$ [equivalent to the quantum spin Ising model] we consider $P=2$ modes per site and apply 13 iterations of the RG transformation, so that a final effective site (with just $P=2$ modes) corresponds to $2 \times 2^{13} = 16\,384$ modes of the original system. At the critical point $\lambda=1$, which is the most demanding, the mixedness of the removed modes is at most $\epsilon_r = 1.2 \times 10^{-4}$. The effect on local observables, even after the 13 iterations, is remarkably small: the error in the critical ground-state energy is less than 10^{-7} , while the two-point correlators $\langle a_r^\dagger a_s \rangle$, reconstructed from the MERA, accumulate a relative error that ranges from 10^{-7} for nearest neighbors to 10% for $|r-s| \approx 4000$. Had we not used disentanglers, the error in the energy would be 10^{-3} after only a single RG transformation and an error of 10% in the two-point correlators is already achieved for $|r-s|=42$. (ii) The line $\gamma=0$ (equivalent to the quantum spin XX model) is critical for $|\lambda| < 1$. Here we consider $P=4$ modes per site and apply again 13 iterations of the RG transformation, reaching sizes of $4 \times 2^{13} = 32\,768$ modes. The errors in energy and correlators are similar to those in the line $\gamma=1$. In both cases, an analysis of the RG flow and its fixed points in terms of entanglement is quite insightful, see Fig. 2. ER can also be used to generate a RG transformation in the space of Hamiltonians by replacing Eq. (10) with a minimization of the energy. Figure 3 shows that critical systems are also fixed points of this alternative approach that preserves the low energy spectrum.

In 2D the model has three phases, denoted I, II, and III, where the distinct forms of entanglement scaling were characterized.⁵ In phases II (critical with a Fermi surface consisting of a finite number of points) and III (noncritical with a gap in the energy spectrum) we are once more able to coarse grain the system in a quasixact, sustainable manner. This is remarkable. The entropy of a square block made of L^2 modes grows as the size of its boundary,⁵ $S_L \sim L$. This implies that the number of modes we should keep in an effective site grows *exponentially* with the number of iterations of the RG transformation, which is precisely why DMRG does not work for large 2D systems. Instead, disentanglers bring this number again down to just a *constant*. As a result one can, in principle, explore systems of arbitrary sizes. In particular, by considering $P=4^2$ modes per site we apply $\tau=4$ iterations of the RG transformation, with a final block effectively spanning $P \times 4^{\tau+1} = 16\,384$ modes, while maintaining truncation errors of the same scale as the 1D models analyzed, $\epsilon_r = 1.1 \times 10^{-4}$. As in the 1D case, the structure of fixed points of the RG flow can be understood in terms of the

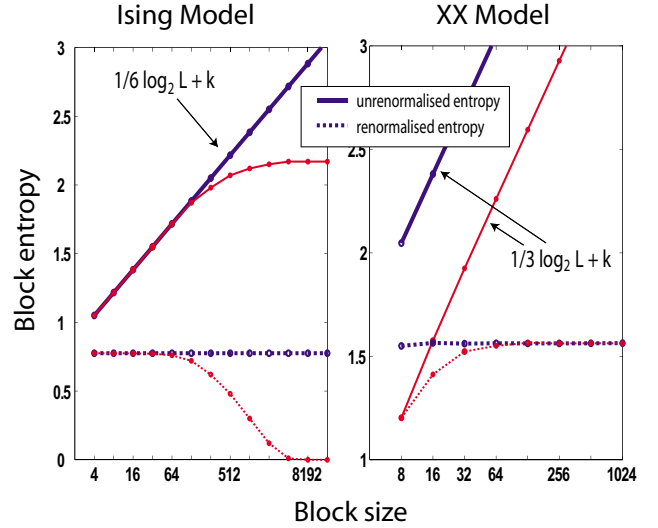


FIG. 2. (Color online) Scaling of the entanglement entropy S_L (Ref. 10) in 1D systems. Left: quantum Ising model, $\gamma=1$. Bold (solid and dotted) lines represent entanglement at criticality, $\lambda=1$. The system is an entangled fixed point of our RG transformation: the correlation matrices $\{\Gamma^{(1)}, \Gamma^{(2)}, \dots\}$ quickly converge to a fixed Γ_{Ising}^* . In particular, the renormalized entanglement of a block is constant. Thin lines correspond to a noncritical system, $\lambda=1.001$, which the RG flow, as generated by ER, eventually brings a product (unentangled) ground state. Right: quantum XX model, $\gamma=0$. Bold and thin lines represent two critical cases, $\lambda=0$ and $\lambda = \cos(15\pi/16)$. They belong to the same universality class and are found to indeed converge to the same correlation matrix Γ_{XX}^* (with $\Gamma_{XX}^* \neq \Gamma_{\text{Ising}}^*$) and in particular to the same renormalized entropy.

renormalized entanglement, see Fig. 4. On the other hand, phase I (critical, with a one-dimensional Fermi surface) is so entangled that ER is no longer able to prevent the growth in the number P' of modes that need to be kept per site. The system displays a logarithmic correction to the entropy,^{5,6,8} $S_L \sim L \log_2 L$, while the MERA can only reproduce a linear scaling,⁷ $S_L \sim L$, if just a constant number of modes are kept per site, $P'=P$.

V. CONCLUSIONS

We have presented, in the simplified context of fermion models with a quadratic Hamiltonian, unambiguous evidence of the validity of the ER approach in 1D and 2D systems. Similar derivations can be also conducted for bosonic lattice systems with quadratic Hamiltonians.⁹ Our results show that the MERA (Ref. 7) is an efficient description of certain 2D ground states. A number of examples also confirm that (i) ER produces a quasixact, real-space RG transformation where the coarse-grained lattice is locally equivalent to the original one, enabling the study of RG flow both in the space of ground states and Hamiltonians; (ii) noncritical systems end up in a stable fixed point of this RG flow, where the corresponding ground state is a product (i.e., fully disentangled) state, whereas scale invariant critical systems end up in an unstable fixed point, with an entangled ground state. Moreover, ER sheds new light into the ground-state structure of

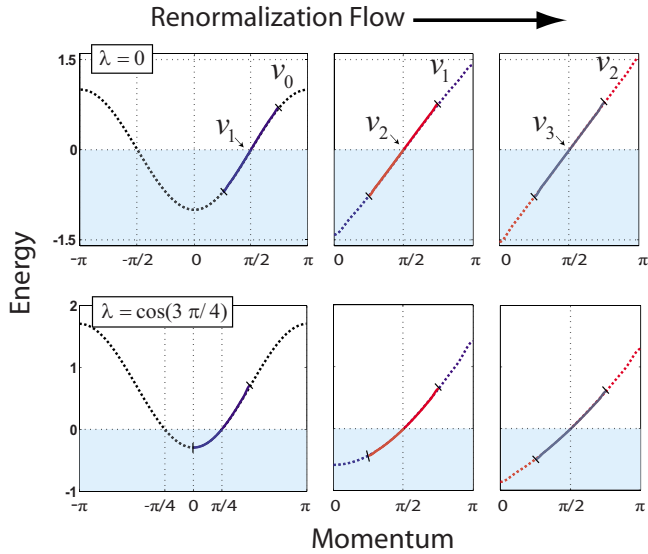


FIG. 3. (Color online) Dispersion relation of Hamiltonian (1) in 1D with $\gamma=0$, the quantum spin XX model, under successive RG transformations. Shading indicates the Fermi sea. A sequence of local, coarse-grained Hamiltonians is obtained $\{H^{(1)}, H^{(2)}, \dots\}$ with their corresponding dispersion relations $\{\nu_1, \nu_2, \dots\}$ converging to a straight line, a fixed point of the RG flow. Convergence is achieved very quickly at half filling ($\lambda=0$) and slower for $\lambda=\cos(3\pi/4)$. These results have been obtained by minimizing the energy while keeping eight modes in each effective site.

two-dimensional systems with a one-dimensional Fermi surface. There, the presence of logarithmic corrections in the entropy S_L of a large block^{5,6,8} cannot be accounted for with the MERA with constant number of modes P per level of coarse graining, hinting for the need for a generalized MERA in order to properly describe such systems.

Recently algorithms for entanglement renormalization in 2D systems of *interacting* particles have been proposed and demonstrated both for spins/bosons^{11–13} and fermions.¹⁴ In particular, the fermionic MERA algorithms¹⁴ are very valuable in that they also allow to study interacting fermions, which typically remain intractable with Monte Carlo sampling techniques due to the so-called *sign problem*. However, the computational cost of implementing these more general MERA algorithms scales as a large power of the MERA bond dimension χ (which is related to the modes per site parameter P used in this work as $\chi=2^P$). The high computational cost associated to the general algorithms¹⁴ for interact-

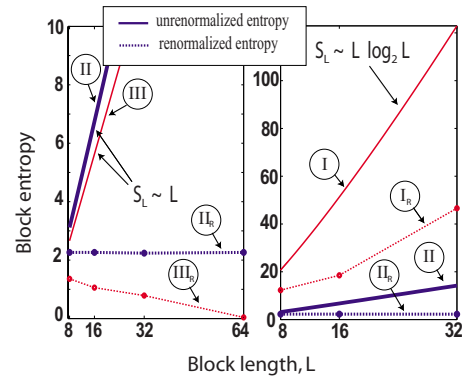


FIG. 4. (Color online) Entanglement entropy S_L of a block of $L \times L$ modes in 2D models. Left: in the critical phase II and the noncritical phase III (bold and fine lines, respectively) the entanglement entropy grows linearly with the size L of the boundary of the block, $S_L \sim L$ (boundary law). As in 1D, the renormalized entanglement is constant for the critical model and it eventually vanishes for the noncritical model. We have considered $\gamma=1$ and $\lambda=2$, $\lambda=2.05$ for the critical and noncritical cases. Right: the critical phase II system $(\gamma, \lambda)=(1, 2)$ is replotted for comparison against critical phase I, $(\gamma, \lambda)=(0, 0)$, where the system has a 1D Fermi surface and the entanglement entropy has a logarithmic correction, $S_L \sim L \log_2 L$. Here disentglers are not able to reduce the renormalized entanglement down to a constant.

ing systems means that in practice only small values of χ can be considered. In the present work, by exploiting the properties of free fermions, we have been able to use values of P which equate to very large values of χ and thus have been able to accurately coarse-grained types I, II, and III phases of 2D fermionic systems with entanglement renormalization. By analyzing the entanglement entropy scaling in each of these phases, as shown Fig. 4, we have been able to gauge the relative difficulty of simulating each type of phase. This is a useful guide for the new fermionic algorithms¹⁴ as it gives us an indication of which systems may be simpler or harder to simulate. We expect it to also be useful in the future development of tensor network algorithms, for instance, by suggesting improvements in the algorithms¹⁴ required to tackle more difficult fermionic problems, such as a type II or type III phase.

ACKNOWLEDGMENTS

The authors thank J. Fjaerestad and R. Orus for comments. Financial support of the Australian Research Council (APA and Grant No. FF0668731) is acknowledged.

¹M. E. Fisher, *Rev. Mod. Phys.* **70**, 653 (1998).

²L. P. Kadanov, *Physics* (Long Island City, N.Y.) **2**, 263 (1966).

³S. R. White, *Phys. Rev. Lett.* **69**, 2863 (1992); *Phys. Rev. B* **48**, 10345 (1993).

⁴G. Vidal, *Phys. Rev. Lett.* **99**, 220405 (2007).

⁵W. Li, L. Ding, R. Yu, T. Roscilde, and S. Haas, *Phys. Rev. B* **74**, 073103 (2006).

⁶T. Barthel, M.-C. Chung, and U. Schollwock, *Phys. Rev. A* **74**,

022329 (2006).

⁷G. Vidal, *Phys. Rev. Lett.* **101**, 110501 (2008).

⁸M. M. Wolf, *Phys. Rev. Lett.* **96**, 010404 (2006); D. Gioev and I. Klich, *ibid.* **96**, 100503 (2006).

⁹G. Evenbly and G. Vidal, *New J. Phys.* **12**, 025007 (2010).

¹⁰G. Vidal, J. I. Latorre, E. Rico, and A. Kitaev, *Phys. Rev. Lett.* **90**, 227902 (2003); J. I. Latorre, E. Rico, and G. Vidal, *Quantum Inf. Comput.* **4**, 48 (2004).

- ¹¹G. Evenbly and G. Vidal, *Phys. Rev. B* **79**, 144108 (2009).
- ¹²L. Cincio, J. Dziarmaga, and M. M. Rams, *Phys. Rev. Lett.* **100**, 240603 (2008).
- ¹³G. Evenbly and G. Vidal, *Phys. Rev. Lett.* **102**, 180406 (2009); **104**, 187203 (2010).
- ¹⁴P. Corboz, G. Evenbly, F. Verstraete, and G. Vidal, *Phys. Rev. A* **81**, 010303(R) (2010); C. Pineda, T. Barthel, and J. Eisert, [arXiv:0905.0669](https://arxiv.org/abs/0905.0669) (unpublished); P. Corboz and G. Vidal, *Phys. Rev. B* **80**, 165129 (2009); T. Barthel, C. Pineda, and J. Eisert, *Phys. Rev. A* **80**, 042333 (2009).